## SPACE SCIENCES

# The source craters of the martian meteorites: Implications for the igneous evolution of Mars

Christopher D. K. Herd[1]*, Jarret S. Hamilton[1]†, Erin L. Walton[2]‡, Livio L. Tornabene[3,4], Anthony Lagain[5,6,7], Gretchen K. Benedix[5,8,9], Alex I. Sheen[1,10,11], H. J. Melosh[12,13]§, Brandon C. Johnson[12,13], Sean E. Wiggins[12,14], Thomas G. Sharp[15], James R. Darling[16]

Approximately 200 meteorites come from ~10 impact events on the surface of Mars, yet their pre-ejection locations are largely unknown. Here, we combine the results of diverse sets of observations and modeling to constrain the source craters for several groups of martian meteorites. We compute that ejection-paired groups of meteorites are derived from lava flows within the top 26 m of the surface. We link ejection-paired groups to specific source craters and geologic units, providing context for these important samples, reconciling microscopic observations with remote sensing records, and demonstrating the potential to constrain the ages of their source geologic units. Furthermore, we show that there are craters that may have produced martian meteorites not represented in the world's meteorite collections that have yet to be discovered.

## INTRODUCTION

The majority of martian meteorites comprise a suite of mafic to ultramafic igneous rocks, formed during eruption of magmas at or near the surface of Mars (1, 2). They represent ~200 rocks, grouped on the basis of similarities in their petrological characteristics ["pairing groups;" (1)]. Over 80% by number belong to the shergottite subgroup, a suite of tholeiitic igneous rocks that were emplaced as lava flows within the past ~600 million years (Ma) (1). The remainder belongs to subgroups that can be divided on the basis of their radiometric ages: the ~1350-Ma nakhlites and chassignites (3), the ~2400-Ma augite-rich shergottites (4, 5), the ~4100-Ma Allan Hills (ALH) 84001 orthopyroxenite (6), and the Northwest Africa (NWA) 7034 meteorite and its petrologic pairs. The latter is a regolith breccia containing clasts of a variety of types with minerals as old as 4480 Ma, assembled within the past ~1500 Ma (7, 8). The representation of ages within the martian meteorites is at odds with the ages of Mars' surface geologic units mapped using remote sensing data and determined through crater counting, via extension of the lunar cratering record (9): ~75% of the surface of Mars is Hesperian to Noachian (>~3400 Ma), whereas only one-quarter of the martian surface is younger in age, belonging to the Amazonian (10). This apparent paradox is resolved by the process through which the martian meteorites are formed: The impact of a bolide onto the surface of Mars causes material near the point of impact to be accelerated faster than the 5 km/s escape velocity, allowing a proportion of the ejected material to enter into Earth-crossing orbits (11, 12). Ejection of material can occur from impact events that form craters as small as ~3 km diameter (11). While there are an estimated 80,000 craters of that size on Mars (13, 14), it is now understood that only impacts into surface units that have a relatively high competency would enable the ejection of material (15–17); thus, the impact ejection process acts as filter and biases the suite of martian meteorites toward young, relatively unaltered, unbrecciated igneous rocks (18–20). This bias in composition may explain the differences between martian meteorites and igneous rocks analyzed at the surface; these two groups of rocks appear to be derived from distinct mantle sources (2). Of the martian meteorites, only the regolith breccia has a bulk composition similar to surface rocks (2); accordingly, its source may be in the southern highlands (21).

Cosmic ray exposure (CRE) data enable the timing of ejection of martian meteorites to be constrained, assuming that the CRE age (or the CRE age + the terrestrial age, where applicable) represents the timing of the impact event that ejected material from the martian surface. This assumption is supported by the observation that in the majority of the most highly shocked martian meteorites (i.e., the shergottites); the homogeneity and type of shock damage indicate a single shock event, most likely the event associated with ejection (19). Meteorites with similar petrography and/or geochemical characteristics tend to have the same ejection age (2, 22). A notable example is a group of >10 shergottites that are depleted in incompatible trace elements and which share a 1.1 Ma ejection age (5). All of the nakhlites and chassignites appear to have been ejected in a single event at 11.5 ± 2.1 Ma (23). On the basis of similarities in CRE and crystallization age, the martian meteorites represent 10 ejection-paired groups, with ejection ages ranging between 0.6 and 20 Ma (fig. S1 and data S1). The goal of our study is to link the eight ejection-paired groups of Amazonian meteorites (i.e., excluding ALH 84001 and NWA 7034 and pairs) to specific source craters.

[1]Department of Earth and Atmospheric Sciences, University of Alberta, Edmonton, AB T6G 2E3, Canada. [2]Department of Physical Sciences, MacEwan University, Edmonton, AB T5J 4S2, Canada. [3]Department of Earth Sciences, Institute for Earth and Space Exploration, University of Western Ontario, 1151 Richmond Street, London, Ontario N6A 5B7, Canada. [4]The SETI Institute, 339 Bernardo Ave, Suite 200, Mountain View, CA 94043, USA. [5]Space Science and Technology Centre, School of Earth and Planetary Sciences, Curtin University, Bentley, Western Australia, Australia. [6]Aix-Marseille Université, CNRS, IRD, INRA, CEREGE, Aix en Provence, France. [7]Institut ORIGINES, Aix-Marseille Université, Marseille, France. [8]Planetary Science Institute, Tucson, AZ 85719, USA. [9]Department of Earth and Planetary Sciences, Western Australia Museum, Perth, Western Australia, Australia. [10]Royal Ontario Museum, 100 Queens Park, Toronto, ON M5S 2C6, Canada. [11]Department of Earth Sciences, University of Toronto, Toronto, ON M5S 3B1, Canada. [12]Department of Earth, Atmospheric, and Planetary Sciences, Purdue University, West Lafayette, IN 47907, USA. [13]Department of Physics and Astronomy, Purdue University, West Lafayette, IN, USA. [14]Lawrence Livermore National Laboratory, Livermore, CA 94550, USA. [15]School of Earth and Space Exploration, Arizona State University, Tempe, AZ 85287-1404, USA. [16]School of the Environment, Geography and Geosciences, University of Portsmouth, Portsmouth PO1 3QL, UK.
*Corresponding author. Email: herd@ualberta.ca
†Present address: Environment and Climate Change Canada, 9250 49 St. NW, Edmonton, AB T6B 1K5, Canada.
‡Deceased.
§Deceased.

Previous attempts to determine the sources of the martian meteorites have met with limited success. The 55-km-diameter crater Mojave, located in ~4300-Ma Xanthe Terra, has been suggested as the source of several shergottite meteorites (Shergotty, Los Angeles, and Queen Alexandra Range 94201) and ALH 84001 (24); however, it is unlikely that Mojave crater would generate meteorites with a wide range of CRE and formation ages (23). Spectral matching has been the basis for other studies linking the meteorites to martian surface units [e.g., (25)]. This approach is hindered by extensive dust cover, especially on younger terrains such as Tharsis and Elysium (26, 27), as well as the nonunique visible/near-infrared spectral characteristics of the meteorites with respect to the composition of the martian surface. Furthermore, surface units of a wide range of ages, at least into the Hesperian, contain igneous minerals similar to those found in the meteorites (25, 27). It is perhaps expected, therefore, that spectral matches to martian meteorites tend to occur in relatively dust-free, Hesperian to Noachian terrains (25). In contrast, Mouginis-Mark et al. (28) suggested that shergottites and nakhlites, as young, igneous rocks, are derived from the (Amazonian-aged) Tharsis region, on the basis of a much more limited martian meteorite inventory than currently available and only nascent modeling of the impact ejection process. That the source craters of the now ~200 martian meteorites formed very recently and lie on Amazonian igneous terrain is evident by the fact that they are predominantly young, igneous rocks ejected within the past 20 Ma.

The remote sensing observations of impact craters by (29, 30) demonstrate that the presence of primary crater-fill deposits (e.g., pitted impact melt-bearing units) can be used as a criterion for degree of crater preservation, in addition to the presence of thermally contrasted ejecta or rays, which consist of dense clusters of secondary craters ("secondaries"), formed during impact by ballistic ejection of material traveling at sub-escape velocity (31). Thus, while considering the rates of degradation (erosion and burial) on Mars, a crater is considered to have formed recently if it preserves such primary crater-fill deposits, and rays comprised of small ($D \lesssim 100$ m)

secondaries (21, 29–31). Advances in machine learning have facilitated the use of crater counting methods to determine the ages of surface units on Mars; the crater detection algorithm (CDA) of (32) has been used to successfully reproduce the manually counted database of (13) and to routinely determine robust surface ages (33, 34). The algorithm has also been used in the effort to determine martian meteorite source craters: application of the CDA to craters in the Context Camera global mosaic [beta01 release; (35)] by (36) generated a database of ~94 million craters and validated the use of secondaries as a criterion for identifying recent impact craters, thus complementing studies that highlight thermally contrasted ejecta or rays to identify potential martian meteorite source craters (31). The study of (36) identified 19 craters >3 km diameter that could be the sources of martian meteorites and linked the group of depleted olivine-phyric shergottites ejected at 1.1 Ma to two potential source craters in Tharsis: Tooting and Chakpar [ID 09-000015; (13)]. Similarly, Karratha crater, formed 5 to 10 Ma ago within the ejecta blanket of the 1.5-billion-year (Ga) crater Khujirt, was identified as the source crater for the regolith breccia NWA 7034 and its lithologic pairs, by linking the crater's age and surrounding terrain characteristics to the multistage history of the meteorite (21). Here, we capitalize on advances in modeling, remote sensing, and crater chronology methods to place constraints on the source craters of the ejection-paired meteorite groups that exhibit Amazonian crystallization ages and test the conclusions of previous studies.

## RESULTS

Recently, forward models of the shock conditions of material ejected from Mars were obtained using high-resolution simulations of impacts into a Mars-like basaltic target (37). Here, these model results are co-inverted for peak shock pressures and dwell time (duration of an ejected rock at peak shock pressure) obtained from analysis of shock features in the meteorites (Table 1; also, Materials and Methods). These results are used to infer a range of impact crater diameters

**Table 1. Ages, conditions of impact ejection, and modeling results for selected martian meteorites.** $T_{crys}$: igneous crystallization age; $T_{ej}$: ejection age; group: ejection-paired group (23). Ages, dwell times, and peak shock pressures are provided in Materials and Methods. Effective crater diameter range is the model-derived crater diameter adjusted for 45° impact angle (see Materials and Methods). In the case of Chassigny and NWA 8159, the lower limit is the minimum diameter of a crater that could eject material, following (11). Pre-impact burial depth depends on the diameter of the crater (effective diameter); see data S2 (23) for specific values. The range is shown here. N is the number of candidate craters in the effective crater diameter range in Amazonian igneous terrains.

| Meteorite | $T_{crys}$ (Ma) | $T_{ej}$ (Ma) | Group | Model input | | Model output | | | | | Candidate crater source (burial depth) |
| | | | | Dwell time (ms) | P, bulk (GPa) | Impactor radius (m) | Crater diameter range (model, km) | Effective crater diameter range (km) | Burial depth (model, m) | N | |
|---|---|---|---|---|---|---|---|---|---|---|---|
| **EETA79001** | $173 \pm 10$ | $0.6 \pm 0.1$ | 1 | 10 | $36 \pm 5$ | 549–1786 | 16–46 | 8–46 | 3.75–17.2 | 10 | Chakpar (7.88 m) |
| **Zagami** | $177 \pm 3$ | $2.9 \pm 0.2$ | 4 | 10 | 22–23 | 781–1250 | 22–33 | 11–33 | 1.4–5.23 | 8 | Corinto (1.57 m) |
| **Los Angeles** | $170 \pm 8$ | $2.9 \pm 0.5$ | 4 | 10–20 | 29–31 | 685–7692 | 19.6–165 | 9.8–165 | 1.79–8.21 | 10 | Corinto (2.47 m) |
| **Tissint** | $574 \pm 20$ | $1.1 \pm 0.1$ | 2 | 10–20 | $\geq 29$ | 407–7692 | 12.4–165 | 6.2–165 | 4.62–36.6 | 11 | Tooting (26.1 m) |
| **Chassigny** | $1340 \pm 50$ | $11.3 \pm 0.6$ | 7 | 1–10 | 26–32 | 63–3846 | 2.41–89 | 3–89 | 0.37–9.70 | 15 | Kotka (9.7 m) |
| **NWA 8159** | $2370 \pm 250$ | $1.2 \pm 0.2$ | 3 | 100* | 15–23 | 7246–41667 | 156–728 | 3–728 | 0.2–5.23 | 15 | Domoni (1.64 m) |

*Dwell time for NWA 8159 is considered an upper limit; for this reason, the effective minimum crater diameter could be as low as the minimum that could eject material.

that would have ejected material with the observed meteorite shock features. Notably, the model results also provide constraints on pre-impact burial depth. Although our estimates of burial depth have significant uncertainty (Materials and Methods), we assess whether these estimates can be reconciled with the local geology of potential source craters and the petrology and absolute or relative age of each meteorite.

We assign the six meteorites included in our study, Elephant Moraine (EET) A79001, Zagami, Los Angeles, Tissint, Chassigny, and NWA 8159 (Table 1), to five ejection-paired groups, on the basis of CRE age (data S1) (23). These five distinct ejection events correspond to over half of the events responsible for all of the known Amazonian martian meteorites (23). Model ages of crater candidates and their surrounding terrain compared to the CRE ages and crystallization ages of martian meteorites (Fig. 1) are used to link specific meteorite groups to specific craters (Fig. 1). A map of most likely crater source locations is given in Fig. 2.

On the basis of a distinct and resolvable ejection age, we infer that EETA79001 was ejected in a unique event [group 1; (23)] and thus comes from a separate source crater with a model age of ~0.6 Ma and a unit age of 170 Ma. No candidate craters meet these criteria; however, Chakpar crater is a 19.6 km diameter crater located on the Tharsis plateau, ~500 km northeast of Ascraeus Mons, with a crater formation model age of $0.429^{+0.11}/_{-0.091}$. This crater is marked by a ~3-km-wide younger lava flow that emanates from beneath the crater's ejecta. The age of the lava flow cannot be accurately dated, due to its small surface area and contamination by secondaries from Chakpar; however, its age is younger than the surrounding terrain, which has a model age of 542 ± 83 Ma. Therefore, the lava flow

could be the source of EETA79001, which would be derived from the upper 7.9 m from a crater of this size (Table 1).

Tissint is interpreted to have been a flow that was buried before impact ejection at 1 Ma, along with the other members of this ejection-paired group (5), the youngest, and presumably topmost, member of which is NWA 1195, with an age of 348 Ma [group 2; (23)]. Thus, the source crater for this group should have a model age close to 1 Ma and a unit age of ~350 Ma. As noted by (36), the most likely source crater is Tooting, although crater Chakpar is an alternative source, within uncertainties. The estimated pre-impact burial depth of Tissint for a crater the size of Tooting is 26.1 m (or 16.8 m if the source crater is Chakpar), consistent with Tissint being deeper within a stack of flows.

It is difficult to reconcile the estimated pre-impact burial depth of NWA 8159 with that of Tissint and the other 1-Ma ejected shergottites. We consider the possibility that these were ejected in a separate event [group 3; (23)]. Our impact modeling yields a pre-impact burial depth of at most 5.2 m for NWA 8159 (based on the largest possible impact crater), substantially shallower than that for Tissint (Table 1), even when uncertainties are considered. If NWA 8159 and NWA 7635 were the lowermost flows in the stack, it is difficult to envision as many as a dozen younger flows within a depth of only ~5 m (or <3.7 m if Tooting crater was the source). The only way for NWA 8159 and 7635 to be derived from Tooting crater with the other 1-Ma ejected shergottites is if there were multiple lava flows near the surface that range in age from 2400 to ~350 Ma; this is unlikely based on mapping (38).

The source crater for the augite-rich shergottites should have a model age of 1 Ma and a unit age of ~2400 Ma. Several candidate
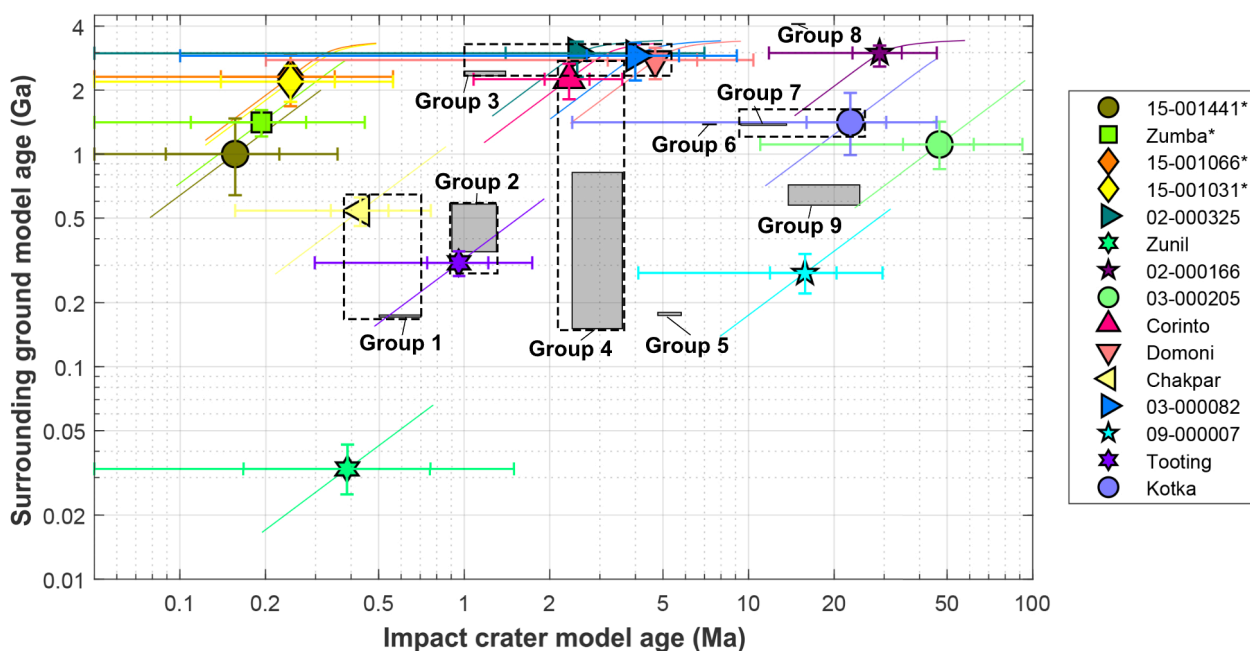


**Fig. 1. Model ages of the crater candidates and their surrounding ground compared to the range of CRE and crystallization ages of martian meteorite groups.** Impact craters in the legend are sorted by size and the impact model age of the four smallest craters (*) are from the recurrence formation interval, assuming they are the youngest of their size formed on the martian surface (23). Error bars are generated from crater counts and the wider uncertainties for the impact model age account for an arbitrary factor of 3 in the statistical uncertainties (see Materials and Methods). As in (36), oblique lines illustrate the expected model ages' deviation if different cratering rates are considered: ± a factor of 2 around the chronology function from (44). Meteorite groups that are linked to specific craters are shown with dashed boxes: group 1 = Chakpar; group 2 = Tooting; group 3 = Domoni; group 4 = Corinto; and group 7 = Kotka; see also data S3.
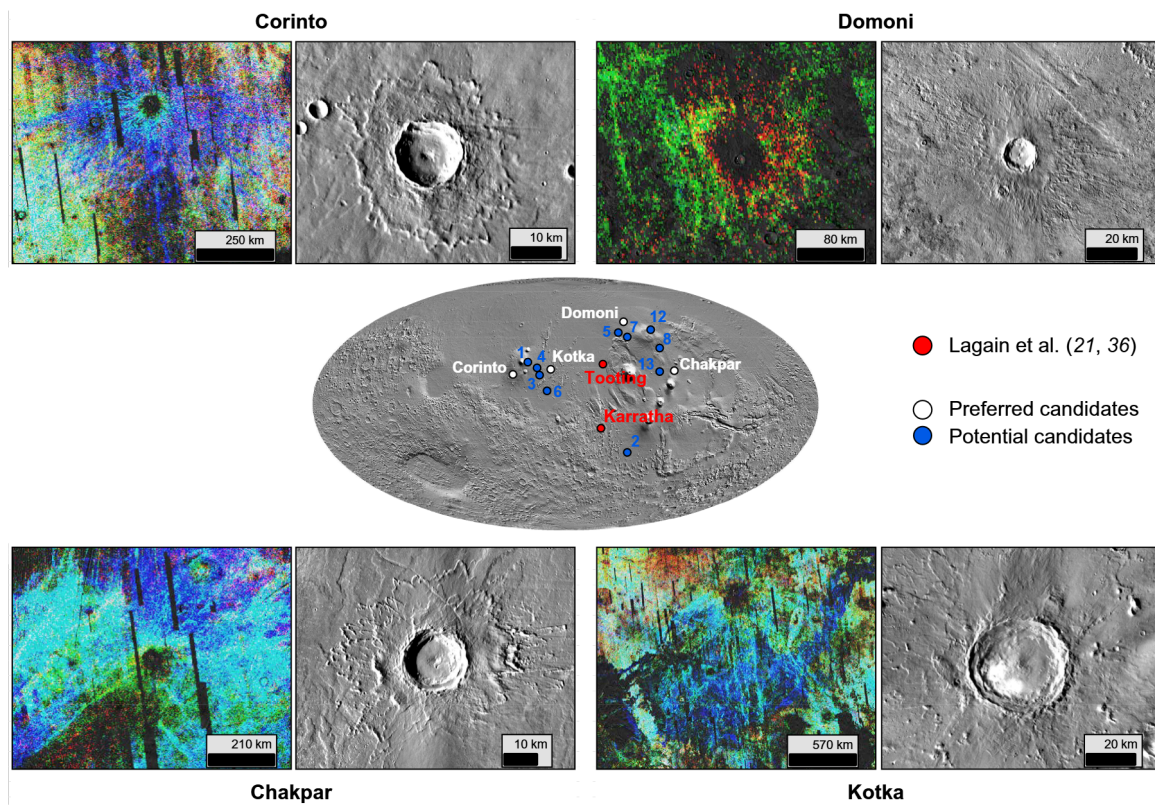
**Fig. 2. Location of the crater candidates for the ejection sites of martian meteorites.** Red points denote the craters proposed for the launch of depleted olivine-phyric shergottites ejected 1.1 Ma ago and the regolith breccia: Tooting (*36*) and Karratha (*21*), respectively. Background: Mars Orbital Laser Altimeter shaded relief. White dots mark the preferred candidates discussed in this study; blue dots are well-preserved craters and potential candidates for the ejection of material that cannot be linked to any currently known meteorites. The four preferred candidates (except Tooting) are shown individually. For each crater, the left is the crater density distribution detected by the CDA (*32*, *33*, *36*); colors indicate crater densities of specific diameter range (blue, 25 to 75 m; green, 75 to 150 m; and red, 150 to 300 m). The right of each is a close-up showing each crater on daytime Thermal Infrared Imaging System data.

source craters [unnamed; IDs from (*13*)] have unit ages that overlap: 15-001066 ($2310^{+600}/_{-630}$ Ma), 15-001031 ($2190^{+410}/_{-430}$ Ma), and 02-000325 ($2980^{+400}/_{-670}$ Ma); likewise, Domoni has a unit age of $2770^{+390}/_{-520}$, within uncertainties of the crystallization age of these meteorites. Craters 15-001066, 15-001031, and 02-000325 have weak or no secondary elements (data S2); this and their small size reduce the likelihood that they generated meteorites. Domini is located on the NW flank of Alba Mons; its model age is $4.7^{+1.9}/_{-1.5}$ and its recurrence interval age is 1.487 Ma. Whereas these are old relative to the ejection ages of NWA 7635/8159, the prominent secondaries and thermal elements make this crater the most likely candidate (*23*). The modeled pre-impact burial depth of only 1.64 m for NWA 8159 (Table 1) from this crater implies that the unit at the surface would be representative of the augite-rich shergottite lithology. Spectral classification a dust-free area on the north flank of Alba Mons is consistent with a high-calcium pyroxene (augite-rich) signature (*27*).

We interpret Zagami and Los Angeles to be within a stack of flows that is represented by the 56 shergottites ejected at 3.0 ± 0.6 Ma [group 4; (*23*)]. Although a large ejection-paired group, most (19 of 25) crystallization ages from this group are between 151 and 224 Ma. Thus, the crater that ejected Zagami, Los Angeles, and its ejection pairs should have a model age of 3 Ma and a unit age of ~200 Ma, although the unit age could be younger if there were a number

of flows on top of this group. None of the candidate craters that we identified fit these criteria. The closest possible match is 13.5-km-diameter Corinto (model age of 2.34 ± 0.42 Ma), located in Elysium Planitia, ~500 km SW of Elysium Mons and Albor Tholus. Corinto has one of the most extensive crater ray systems on Mars (*36*, *39*), extending over 2000 km, suggesting that a relatively large volume of material was ballistically ejected. However, the unit age for Corinto is $2250^{+410}/_{-440}$ Ma (data S2). This crater could be the source, if the crater happened to sample a younger set of flows on an older surface; an inference supported by mapping of the crater and surrounding area (*40*). The estimated pre-impact burial depths for Zagami and Los Angeles from a crater the size of Corinto are only 1.57 and 2.47 m, respectively. Thus, the meteorites would be derived from lava flows very near the surface.

Chassigny is considered to be part of the same event that ejected all of the chassignites and nakhlites; the source crater for this ejection-paired group should have a model age close to 11 Ma and a unit age of ~1400 Ma [group 7; (*23*)]. Kotka, which has a unit model age of $1410^{+530}/_{-420}$ Ma is the most likely source. While the crater's model age ($23^{+8}_{-6}$ Ma) is too old by a factor of two (*36*), there are large uncertainties on the model age due to the small number of craters used to derive the model age (*n* = 10), the potential presence of autosecondaries, and the sensitivity of the crater diameter to the target properties (*41*). A large number of secondaries are associated with

Kotka, up to about 1500 km distance, consistent with (suborbital) ballistic trajectories of ejecta blocks; furthermore, preserved secondaries suggest that the crater's model age is overestimated. The complex history of the terrain and the rampart ejecta blanket suggesting the presence of volatiles in the target is consistent with the aqueous alteration recorded in the nakhlites (42). The model-based pre-impact burial depth is 9.7 m (Table 1); while still shallow if the rock was once part of a larger igneous complex, we consider this crater the most likely candidate.

Our results have implications for the sources of other ejection-paired groups of martian meteorites; these are provided in (23). Refinement of these sources would require constraints from dwell time estimates and impact ejection modeling.

## DISCUSSION

Our approach has enabled the identification of candidate source craters for four of the at least six source craters for the shergottite meteorites, in addition to the single source crater for the nakhlites/chassignites. Two of the source craters are located in Elysium, and three in Tharsis (Fig. 2). Corinto (Elysium) appears to be the source of geochemically enriched shergottites, whereas Chakpar and Tooting (Tharsis) are sources of intermediate and depleted shergottites, respectively (data S3). This result has implications for the interpretation of the mantle sources for the martian meteorites: The more geochemically enriched mantle component may be more prevalent under Elysium and less involved in magmagenesis under Tharsis. Linking other geochemical and ejection-paired groups (data S3) to crater sources in these volcanic regions would test this hypothesis.

There appear to be several craters included in our study from which no known martian meteorites have yet been identified (data S2). This includes crater 02-000166, on a terrain with an age of $2990^{+250}/_{-410}$ Ma, an age not represented among those martian meteorites for which crystallization ages have been determined. It is possible that these craters did not source any material, or at least, no material that has yet been discovered or dated. The bias in sampling among the martian meteorites toward younger, predominantly igneous rocks, is attributable to the impact delivery process, which preferentially samples more competent units (17, 19). Terrains that are older have been subject to more fracturing due to impact cratering events and are more likely to have been affected by aqueous alteration (19). Zunil, which is located in the southeast corner of Elysium Planitia within Cerberus Fossae, has a model age of $0.4^{+0.4}/_{-0.2}$ Ma and sits on a unit with an age of $33^{+10}/_{-8}$ Ma (36). It seems likely that material was ejected from this crater; however, its young model age and geologic unit age are not represented in any known meteorites. Given the young model age, and constraints from secular resonance effects (43), perhaps any meteorites from this ejection event have yet to arrive on Earth. An additional factor is the effect of the surface properties; modeling of layering within the target surface suggests that intact lava flows over regolith or cemented sediment would not eject any material above Mars escape velocity (17); in general, intact material must be present to a depth of ~10% of the impact radius (17).

Our results place constraints on the source craters for a number of key martian meteorite groups, and importantly link specific meteorite samples, with known radiometric ages, to igneous surfaces in the Elysium and Tharsis regions of Mars. This enables refinement of the sequence of volcanic events in these regions, the origins of varied mantle source characteristics for martian magmas, and the accumulation rate of craters during the Amazonian history of Mars. Recalibration of the cratering rate for Mars at the current time is not yet possible: While some of the ejection ages are close to the crater model formation age of the source crater, not in all cases is the crystallization age of the meteorite close to the model age of the surrounding terrain. We are unable to assess whether there is a systematic shift in the cratering rate relative to the Hartmann chronology function (44). Nevertheless, additional constraints from impact modeling of meteorites and geologic mapping of potential source craters will enable the recalibration of Mars' chronology, using late and middle Amazonian calibration points, with implications for the timing, duration and nature of a wide range of major events throughout martian history.

## MATERIALS AND METHODS
### Experimental design

We combine constraints from several methods—impact modeling, crater preservation, and crater chronology—to link specific ejection-paired groups of meteorites to specific source craters. We focus on martian meteorites for which dwell times of shock loading have been estimated from petrological constraints and that span most of the observed range of crystallization and ejection ages for meteorites from Mars, representing the most common types: shergottites/augite-rich shergottites and nakhlites/chassignites (Table 1). We review ejection pairings and constrain at least six distinct ejection events for the shergottites, in addition to the single event for the majority of the nakhlites/chassignites (23); these are compiled in data S1. Application of criteria indicative of young impacts (e.g., pitted impact melt-bearing units, thermally contrasted ejecta or rays) yields a database of the 294 best-preserved craters over a range of terrain types and ages (see the "Database of best preserved impact craters" section); a database that we infer to represent craters that formed most recently (<<1 Ga). Selection of the best-preserved craters from this database for those occurring on Amazonian igneous terrains results in a list of 15 candidate source craters that are the most likely sources of material ejected within the past 20 Ma (data S2). Of these, Zunil, Corinto, Chakpar, Tooting, and Kotka overlap with the 19 craters identified by (36); these represent craters that have secondaries of ≲100 m diameter craters on Amazonian igneous surfaces, strongly suggestive of a high degree of preservation (and therefore young in age), and the ejection of blocks of material on ballistic trajectories, some of which may have escaped Mars. Independently, we applied the impact model of (37) to the martian meteorites to yield permissible crater diameters for each meteorite (Table 1). Cross-reference of the range of permissible crater diameters from this modeling with the database of best-preserved craters on Amazonian igneous units demonstrates that all 15 candidate source craters could be the sources of Chassigny and NWA 8159; however, more restricted permissible crater diameters for some meteorites results in a smaller number of possible craters for the other meteorites, including only eight for Zagami (Table 1). To link each of the martian meteorites used in our study (Table 1) to specific source craters, we used the automatic crater database built by (36), completed and corrected by manual crater mapping, to determine the crater formation model ages of the 15 candidate source craters, and the manual database from (14) to derive the ages of the geologic units on which they occur ("unit model ages"). We then compare

those results to the meteorites' ejection and crystallization ages. Model ages are provided in data S2.

The uncertainties on crater counting-derived ages are dependent on the number of craters used in the chronology—fewer craters on a smaller surface area results in larger uncertainties—and uncertainties in the cratering rate (*45–48*). For this reason, when evaluating whether a given ejection-paired group of meteorites may be linked to a specific crater, we consider a match if the CRE age and the crater formation model age agree within a factor of 3. We report the crater formation model ages and the geologic unit ages based on a factor of 2 uncertainty in the cratering rate (*44*).

The impact model is sensitive to pre-impact burial depth. We apply the model to each of the candidate craters for each meteorite, to generate the maximum pre-impact depth. We then assess whether the model ages of the source craters and geologic unit ages can be reconciled with the ejection ages and crystallization ages of the meteorites. Furthermore, we attempt to reconcile our estimate of pre-impact burial depth with the petrology and absolute or relative age of each meteorite.

### Impact modeling
Dwell times and peak pressures (Table 1) are provided from previous studies: EETA79001 dwell time from (*49*) and peak pressure from (*50*); Zagami dwell time and peak pressure from (*51*); Tissint dwell time and peak pressure from (*52*); Chassigny dwell time from (*53*) and peak pressure from (*50*); and NWA 8159 dwell time and peak pressure from (*54*). The dwell time for the Los Angeles meteorite is estimated based on similarities in petrography, relative to EETA79001 and Zagami (*55*). We consider the peak pressure of 45 ± 3 GPa of (*50*), based on the refractive indices of plagioclase glass, to be too high; the shock features (*55*) are more consistent with a lower peak pressure ~30 GPa (as reported in Table 1). This lower peak pressure is also consistent with the work of Hu *et al.* (*56*) that shows a lower transition pressure for the plagioclase-to-maskelynite transition. Furthermore, we note that the range of peak pressures that we used in our study for NWA 8159, which contains partial conversion to maskelynite, encompasses the pressure range of 17.4 to 21.7 GPa reported by Hu *et al.* (*56*).

Using the data of Bowling *et al.* (*37*) for 13 km/s impact velocity, we find the scale dwell times and scale burial depths that correspond to the bulk peak pressures for each meteorite. With the minimum and maximum values of scale dwell time we then find the range of impactor radii for each meteorite by dividing observationally derived dwell time by the scaled dwell times. The burial depth is calculated by multiplying the scaled burial depth range from (*37*) by the impactor size range obtained using the observed dwell time. For a given constraint on the range of shock pressures a meteorite experiences, the scaled burial depth is simply the range of provenance depths where rocks experiencing those shock pressures will be ejected above martian escape velocity. With these values obtained we then use the crater scaling laws of (*57*), which provides the final crater diameters assuming a typical 45° impact angle, an average 13 km/s impact velocity, and simple-to-complex transition diameter of 8 km the size at which terracing occurs (*13, 58*). The model of (*37*) considers only vertical impacts. On the basis of geometry, an oblique impact could enhance the dwell time ejected materials experience, and the minimum crater size needed to eject a meteorite may be roughly half the size of the minimum size estimated assuming vertical impacts. Thus, our effective crater diameter range includes a

minimum crater size that is half of our minimum modeled crater diameter or 3 km in diameter (whichever is larger); the 3 km diameter corresponds to the minimum crater size capable of producing martian meteorites (*11*). Using the results of (*37*), we have also tested the effect of impact velocity by calculating impactor size, crater size, and burial depth for Zagami using impact velocities of 7.5, 13, and 20 km/s (table S1). Both the lower (7.5 km/s) and higher (20 km/s) impact velocities result in substantially larger maximum burial depths and larger maximum impactor sizes. These results come from the complex interplay of constraints on peak pressure and dwell time. However, we can provide heuristic arguments for these differences. In the case of a low-velocity impact, these differences are generally explained by the lower overall peak shock pressures experienced by material ejected at velocities exceeding Mars' escape velocity such that more of the fast ejecta experience low shock pressures consistent with meteorite constraints (*37*). For the higher velocity case, the difference is explained by the larger volume and greater depth of excavation of material ejected above Mars' escape velocity, which leads to larger maximum excavation depth (*37*). If we consider a given crater size the difference between different impact velocities is more modest. We also note that target layering and material heterogeneity within the target can also affect burial depth estimates. If a layer of cemented regolith or sedimentary material covers intact basalt, the burial depths could increase by approximately 30% (*17*). Heterogeneity in the shock caused by material variations could increase or reduce the burial depth by a similar factor (*17*). We argue that uncertainties in dwell time estimates are a larger source of uncertainty than possible variations in impact velocity, impact angle, or variations in target composition. Note that many of these uncertainties can be thought of as deviations from a typical impact scenario or average shock properties. Thus, although all these uncertainties should be carefully considered when interpreting constraints from impact simulations, comparisons between estimated burial depths for different source craters may provide useful insight.

### Database of best preserved impact craters
The updated crater-related pitted material (CRPM) database based on Tornabene *et al.* (*29*) continues to be expanded and is available online (*59*). The database acts as a means of readily identifying the best-preserved craters on Mars, including those with far-traversing secondary ray clusters and possible candidates representing the youngest craters. These distinctive pitted deposits are readily recognized in high-resolution visible images for their characteristic properties, including dense pit clusters that are distinguishable from primary and secondary crater clusters. On the basis of multiple independent works (*29, 60*), CRPM are consistent with primary deposits, likely representing volatile enriched impact melt-bearing deposits. Craters that preserve impact melts are often relatively young in geological terms and not typically subjected to prolonged exposure to weathering, erosion, or other geological processes that could modify or erase the features associated with the immediate aftermath of the impact event. The preservation of these pitted deposits has been shown to correlate with the preservation of the crater itself, the higher the preservation of the deposits, the more the crater lacks overprinting impacts, and the younger the crater is. Means to identify candidate craters that are among the best-preserved and youngest (<<1 Ga) are vitally important for identifying meteorite source craters as the ejection ages of the entire suite of meteorites on Mars is

less than 20 Ma (*22, 61*). The expanded CRPM database currently contains 294 craters spanning ~0.9 to 220 km and are widespread across the globe from 65°S to 65°N with examples on Hesparian- to Amazonian-aged volcanic terrains, but also including Noachian surfaces as well (*59*).

## Meteorites

Elephant Moraine (EETA) 79001 is composed of two distinct igneous lithologies, both of which likely formed as successive volcanic flows which may have the same or similar mantle source (*62*). The crystallization age of EETA79001 is 173 ± 3 Ma; there is no resolvable difference in age between the two lithologies (*22*). Alteration at the surface of Mars before ejection is indicated by studies of glassy impact melt pockets [e.g., (*63*)], suggesting that the rock belonged to a unit close to the martian surface. The weighted average ejection age of EETA79001 is 0.62 ± 0.17 Ma (fig. S1A and data S1) (*23*) and belongs to ejection-paired group 1.

The Zagami meteorite is classified as an enriched mafic fine-intergranular martian igneous rock on the basis of bulk and incompatible trace element characteristics and texture. The crystallization age of the Zagami meteorite, 177 ± 3 Ma, is well constrained through the application of multiple radiogenic systems [e.g., (*64*)]. Zagami has an ejection age of 2.9 ± 0.2 Ma, an age that overlaps with that of at least 26 other shergottites that have an enriched geochemical character (weighted average of 2.6 ± 0.5 Ma) and at least 57 other shergottites of diverse geochemical character (weighted average of 3.0 ± 0.6 Ma) (fig. S1C and data S1) (*23*). Los Angeles has a crystallization age that overlaps with Zagami and belongs to the same 3-Ma ejection age group (group 4; Table 1). This rock has a more evolved (Fe-rich, Cr-poor) composition and coarser texture relative to Zagami (*65*) but has similar enrichment in incompatible trace elements (*1*).

The Tissint meteorite is a depleted permafic olivine-phyric igneous rock, with an age of 574 ± 20 Ma and an ejection age of 1.1 ± 0.1 Ma (Table 1); Tissint belongs to a group of 10 meteorites with an ejection age of 1.1 ± 0.2 Ma (ejection-paired group 2; fig. S1A and data S1) (*23*), that are most likely derived from Tooting or Chakpar crater (*36*). The petrography of Tissint is consistent with emplacement at the surface as a flow or near the surface as a shallow sill [e.g., (*66*)]; like EETA79001, evidence of near-surface alteration before ejection is recorded in Tissint (*67*).

The Chassigny meteorite is an olivine cumulate with a crystallization age of 1340 ± 50 Ma and an ejection age of 11.3 ± 0.6 Ma (Table 1). It belongs to the ejection-paired group at 11.5 ± 2.1 Ma that includes the chassignites and most of the nakhlites (group 7; fig. S1B and data S1) (*23*). Nakhlites are grouped on the basis of similarities in mineral compositions and texture; the concordance in CRE and crystallization ages suggests a comagmatic origin (*42*). The relationship of chassignites to nakhlites is supported by concordant ages, as well as volatile enrichment (*42*); the NWA 8694 meteorite may represent a lithology intermediate to the two groups (*68*). Given the close petrogenetic and age relationships between chassignites and nakhlites, it is likely that a single ejection event is responsible for all of these meteorites, and that the topmost rocks in the nakhlite/chassignite suite [NWA 817, NWA 5790, and MIL 03346 and pairs; (*42*)] are exposed at the martian surface.

NWA 8159 belongs to a subset of shergottites with crystallization ages of ~2400 Ma, and that includes NWA 7635; the two are petrogenetically linked and have ejection ages of 1.2 ± 0.2 Ma (group 3; fig. S1A and data S1) (*23*). The common ejection ages of these rocks with other 1-Ma ejection shergottites as young as 348 Ma has been used to argue for their derivation from the same ejection site, from a stack of sequential, layered lava flows, with NWA 7635 and NWA 8159 (as the oldest lavas) at the base, implying a long-lived magmatic system with changing mantle source compositions (*5, 36*). However, NWA 8159 and 7635 differ texturally and geochemically from the other 1-Ma ejected shergottites, are likely derived from a distinct mantle source (*4, 69*), and likely therefore result from their own magmatic system.

## Supplementary Materials

**The PDF file includes:**
Supplementary Text
Figs. S1 to S3
Table S1
Legends for data S1 to S3
References

**Other Supplementary Material for this manuscript includes the following:**
Data S1 to S3

## REFERENCES AND NOTES

1. A. Udry, G. H. Howarth, C. D. K. Herd, J. M. D. Day, T. J. Lapen, J. Filiberto, What martian meteorites reveal about the interior and surface of Mars. *J. Geophys. Res. Planets* **125**, e2020JE006523 (2020).
2. H. Y. McSween, Petrology on mars. *Am. Mineral* **100**, 2380–2395 (2015).
3. B. E. Cohen, D. F. Mark, W. S. Cassata, M. R. Lee, T. Tomkinson, C. L. Smith, Taking the pulse of Mars via dating of a plume-fed volcano. *Nat. Commun.* **8**, 640 (2017).
4. C. D. K. Herd, E. L. Walton, C. B. Agee, N. Muttik, K. Ziegler, C. K. Shearer, A. S. Bell, A. R. Santos, P. V. Burger, J. I. Simon, M. J. Tappa, F. M. McCubbin, J. Gattacceca, F. Lagroix, M. E. Sanborn, Q.-Z. Yin, W. S. Cassata, L. E. Borg, R. E. Lindvall, T. S. Kruijer, G. A. Brennecka, T. Kleine, K. Nishiizumi, M. W. Caffee, The Northwest Africa 8159 martian meteorite: Expanding the martian sample suite to the early Amazonian. *Geochim. Cosmochim. Acta* **218**, 1–26 (2017).
5. T. J. Lapen, M. Righter, R. Andreasen, A. J. Irving, A. M. Satkoski, B. L. Beard, K. Nishiizumi, A. J. T. Jull, M. W. Caffee, Two billion years of magmatism recorded from a single Mars meteorite ejection site. *Sci. Adv.* **3**, e1600922 (2017).
6. T. J. Lapen, M. Righter, A. D. Brandon, V. Debaille, B. L. Beard, J. T. Shafer, A. H. Peslier, A younger age for ALH84001 and its geochemical link to shergottite sources in Mars. *Science* **328**, 347–351 (2010).
7. F. M. McCubbin, J. W. Boyce, T. Novák-Szabó, A. R. Santos, R. Tartèse, N. Muttik, G. Domokos, J. Vazquez, L. P. Keller, D. E. Moser, D. J. Jerolmack, C. K. Shearer, A. Steele, S. M. Elardo, Z. Rahman, M. Anand, T. Delhaye, C. B. Agee, Geologic history of Martian regolith breccia Northwest Africa 7034: Evidence for hydrothermal activity and lithologic diversity in the Martian crust. *J. Geophys. Res.* **121**, 2120–2149 (2016).
8. W. S. Cassata, B. E. Cohen, D. F. Mark, R. Trappitsch, C. A. Crow, J. Wimpenny, M. R. Lee, C. L. Smith, Chronology of martian breccia NWA 7034 and the formation of the martian crustal dichotomy. *Sci. Adv.* **4**, eaap8306 (2018).
9. G. Neukum, B. A. Ivanov, W. K. Hartmann, Cratering records in the inner solar system in relation to the lunar reference system. *Space Sci. Rev.* **96**, 55–86 (2001).
10. K. L. Tanaka, J. A. Skinner, J. M. Dohm, R. P. Irwin Iii, E. J. Kolb, C. M. Fortezzo, T. Platz, G. G. Michael, T. M. Hare, Geologic map of Mars (USGS, 2014); https://pubs.usgs.gov/publication/sim3292.
11. J. N. Head, H. J. Melosh, B. A. Ivanov, Martian meteorite launch: High-speed ejecta from small craters. *Science* **298**, 1752–1756 (2002).
12. H. J. Melosh, Ejection of rock fragments from planetary bodies. *Geology* **13**, 144–148 (1985).
13. S. J. Robbins, B. M. Hynek, A new global database of Mars impact craters ≥1 km: 1. Database creation, properties, and parameters. *J. Geophys. Res. Planets* **117**, 2011je003966 (2012).
14. A. Lagain, S. Bouley, D. Baratoux, C. Marmo, F. Costard, O. Delaa, A. Pio Rossi, M. Minin, G. K. Benedix, M. Ciocco, B. Bedos, A. Guimpier, E. Dehouck, D. Loizeau, A. Bouquety, J. Zhao, A. Vialatte, M. Cormau, E. Le Conte, F. Schmidt, P. Thollot, J. Champion, J. Martinot, J. Gargani, P. Beck, J. Boisson, N. Paulien, A. Séjourné, K. Pasquon, N. Christoff, I. Belgacem, F. Landais, B. Rousseau, L. Dupeyrat, M. Franco, F. Andrieu, B. Cecconi, S. Erard, B. Jabaud, V. Malarewicz, G. Beggiato, G. Janez, L. Elbaz, C. Ourliac, M. Catheline, M. Fries, A. Karamoko, J. Rodier, R. Sarian, A. Gillet, S. Girard, M. Pottier, S. Strauss, C. Chanon, P. Lavaud, A. Boutaric, M. Savourat, E. Garret, E. Leroy, M.-C. Geffray, L. Parquet, M.-A. Delagoutte,

O. Gamblin, Mars Crater Database: A Participative Project for the Classification of the Morphological Characteristics of Large Martian Craters, in *Large Meteorite Impacts and Planetary Evolution VI*, W. U. Reimold, C. Koeberl, Eds. (Geological Society of America, Colorado, 2021), pp. 629–644.

15. H. J. Melosh, Impact ejection, spallation, and the origin of meteorites. *Icarus* **59**, 234–260 (1984).

16. N. Artemieva, B. Ivanov, Launch of martian meteorites in oblique impacts. *Icarus* **171**, 84–101 (2004).

17. J. R. Elliott, H. J. Melosh, B. C. Johnson, The role of target strength on the ejection of martian meteorites. *Icarus* **375**, 114869 (2022).

18. P. H. Warren, Lunar and martian meteorite delivery services. *Icarus* **111**, 338–363 (1994).

19. E. L. Walton, S. P. Kelley, C. D. K. Herd, Isotopic and petrographic evidence for young Martian basalts. *Geochim. Cosmochim. Acta* **72**, 5819–5837 (2008).

20. W. K. Hartmann, N. G. Barlow, Nature of the Martian uplands: Effect on Martian meteorite age distribution and secondary cratering. *Meteorit. Planet. Sci.* **41**, 1453–1467 (2006).

21. A. Lagain, S. Bouley, B. Zanda, K. Miljković, A. Rajšić, D. Baratoux, V. Payré, L. S. Doucet, N. E. Timms, R. Hewins, G. K. Benedix, V. Malarewic, K. Servis, P. A. Bland, Early crustal processes revealed by the ejection site of the oldest martian meteorite. *Nat. Commun.* **13**, 3782 (2022).

22. L. E. Nyquist, D. D. Bogard, C. Y. Shih, A. Greshake, D. Stöffler, O. Eugster, Ages and geologic histories of Martian meteorites. *Space Sci. Rev.* **96**, 105–164 (2001).

23. Information on materials and methods is available on Science Online.

24. S. C. Werner, A. Ody, F. Poulet, The source crater of martian shergottite meteorites. *Science* **343**, 1343–1346 (2014).

25. A. Ody, F. Poulet, C. Quantin, J. P. Bibring, J. L. Bishop, M. D. Dyar, Candidates source regions of martian meteorites as identified by OMEGA/MEx. *Icarus* **258**, 366–383 (2015).

26. N. P. Lang, L. L. Tornabene, H. Y. McSween, P. R. Christensen, Tharsis-sourced relatively dust-free lavas and their possible relationship to Martian meteorites. *J. Volcanol. Geotherm. Res.* **185**, 103–115 (2009).

27. C. Viviano, S. L. Murchie, I. J. Daubar, M. F. Morgan, F. P. Seelos, J. B. Plescia, Composition of Amazonian volcanic materials in Tharsis and Elysium, Mars, from MRO/CRISM reflectance spectra. *Icarus* **328**, 274–286 (2019).

28. P. J. Mouginis-Mark, T. J. McCoy, G. J. Taylor, K. Keil, Martian parent craters for the SNC meteorites. *J. Geophys. Res. Planets* **97**, 10213–10225 (1992).

29. L. L. Tornabene, G. R. Osinski, A. S. McEwen, J. M. Boyce, V. J. Bray, C. M. Caudill, J. A. Grant, C. W. Hamilton, S. Mattson, P. J. Mouginis-Mark, Widespread crater-related pitted materials on Mars: Further evidence for the role of target volatiles during the impact process. *Icarus* **220**, 348–368 (2012).

30. L. L. Tornabene, W. A. Watters, G. R. Osinski, J. M. Boyce, T. N. Harrison, V. Ling, A. S. McEwen, A depth versus diameter scaling relationship for the best-preserved melt-bearing complex craters on Mars. *Icarus* **299**, 68–83 (2018).

31. L. L. Tornabene, J. E. Moersch, H. Y. McSween, A. S. McEwen, J. L. Piatek, K. A. Milam, P. R. Christensen, Identification of large (2–10 km) rayed craters on Mars in THEMIS thermal infrared images: Implications for possible Martian meteorite source regions. *J. Geophys. Res. Planets* **111**, E10006 (2006).

32. G. K. Benedix, A. Lagain, K. Chai, S. Meka, S. Anderson, C. Norman, P. A. Bland, J. Paxman, M. C. Towner, T. Tan, Deriving surface ages on mars using automated crater counting. *Earth Space Sci.* **7**, e2019EA001005 (2020).

33. A. Lagain, M. Kreslavsky, D. Baratoux, Y. Liu, H. Devillepoix, P. Bland, G. K. Benedix, L. S. Doucet, K. Servis, Has the impact flux of small and large asteroids varied through time on Mars, the Earth and the Moon? *Earth Planet. Sci. Lett.* **579**, 117362 (2022).

34. A. Lagain, K. Servis, G. K. Benedix, C. Norman, S. Anderson, P. A. Bland, Model age derivation of large martian impact craters, using automatic crater counting methods. *Earth Space Sci.* **8**, e2020EA001598 (2021).

35. J. L. Dickson, L. A. Kerber, C. I. Fassett, B. L. Ehlmann, "A Global blended CTX Mosaic of Mars with vectorized seam mapping: A new mosaicking pipeline using principles of non-destructive image editing" in *49th Lunar and Planetary Science Conference* (Texas LPI Contribution, The Woodlands, 2018).

36. A. Lagain, G. K. Benedix, K. Servis, D. Baratoux, L. S. Doucet, A. Rajšić, H. A. R. Devillepoix, P. A. Bland, M. C. Towner, E. K. Sansom, K. Miljković, The Tharsis mantle source of depleted shergottites revealed by 90 million impact craters. *Nat. Commun.* **12**, 6352 (2021).

37. T. J. Bowling, B. C. Johnson, S. E. Wiggins, E. L. Walton, H. J. Melosh, T. G. Sharp, Dwell time at high pressure of meteorites during impact ejection from Mars. *Icarus* **343**, 113689 (2020).

38. P. J. Mouginis-Mark, "Geologic map of tooting crater, Amazonis Planitia region of Mars" (USGS, 2015); https://pubs.usgs.gov/publication/sim3297.

39. M. Golombek, D. Kass, N. Williams, N. Warner, I. Daubar, S. Piqueux, C. Charalambous, W. T. Pike, Assessment of insight landing site predictions. *J. Geophys. Res.* **125**, e2020JE006502 (2020).

40. J. S. Hamilton, "Constraining the source craters of the martian meteorites: Shock analysis and geologic mapping of candidate craters," thesis, University of Alberta, Edmonton, Canada (2021).

41. J. P. Williams, A. V. Pathare, E. S. Costello, C. L. Gallinger, P. O. Hayne, R. R. Ghent, D. A. Paige, M. A. Siegler, P. S. Russell, C. M. Elder, The effects of terrain properties upon the small crater population distribution at Giordano Bruno: Implications for lunar chronology. *J. Geophys. Res.* **127**, e2021JE007131 (2022).

42. F. M. McCubbin, S. M. Elardo, C. K. Shearer, A. Smirnov, E. H. Hauri, D. S. Draper, A petrogenetic model for the comagmatic origin of chassignites and nakhlites: Inferences from chlorine-rich minerals, petrology, and geochemistry. *Meteorit. Planet. Sci.* **48**, 819–853 (2013).

43. B. Gladman, Destination: Earth martian meteorite delivery. *Icarus* **130**, 228–246 (1997).

44. W. K. Hartmann, Martian cratering 8: Isochron refinement and the chronology of Mars. *Icarus* **174**, 294–320 (2005).

45. A. S. Mcewen, E. B. Bierhaus, The importance of secondary cratering to age constraints on planetary surfaces. *Annu. Rev. Earth Planet. Sci.* **34**, 535–567 (2006).

46. N. H. Warner, S. Gupta, F. Calef, P. Grindrod, N. Boll, K. Goddard, Minimum effective area for high resolution crater counting of martian terrains. *Icarus* **245**, 198–240 (2015).

47. A. Lagain, S. Bouley, D. Baratoux, F. Costard, M. Wieczorek, Impact cratering rate consistency test from ages of layered ejecta on Mars. *Planet. Space Sci.* **180**, 104755 (2020).

48. M. C. Palucis, J. Jasper, B. Garczynski, W. E. Dietrich, Quantitative assessment of uncertainties in modeled crater retention ages on Mars. *Icarus* **341**, 113623 (2020).

49. E. L. Walton, Shock metamorphism of Elephant Moraine A79001: Implications for olivine–ringwoodite transformation and the complex thermal history of heavily shocked Martian meteorites. *Geochim. Cosmochim. Acta* **107**, 299–315 (2013).

50. J. Fritz, N. Artemieva, A. Greshake, Ejection of martian meteorites. *Meteorit. Planet. Sci.* **40**, 1393–1411 (2005).

51. P. Beck, P. Gillet, A. El Goresy, S. Mostefaoui, Timescales of shock processes in chondritic and martian meteorites. *Nature* **435**, 1071–1074 (2005).

52. E. L. Walton, T. G. Sharp, J. Hu, J. Filiberto, Heterogeneous mineral assemblages in martian meteorite resulting from a recent small impact event on Mars. *Geochim. Cosmochim. Acta* **140**, 334–348 (2014).

53. J. Fritz, A. Greshake, High-pressure phases in an ultramafic rock from Mars. *Earth Planet. Sci. Lett.* **288**, 619–623 (2009).

54. T. G. Sharp, E. L. Walton, J. Hu, C. Agee, Shock conditions recorded in NWA 8159 martian augite basalt with implications for the impact cratering history on Mars. *Geochim. Cosmochim. Acta* **246**, 197–212 (2019).

55. E. L. Walton, J. G. Spray, Mineralogy, microtexture, and composition of shock-induced melt pockets in thi Los Angeles basaltic shergottite. *Meteorit. Planet. Sci.* **38**, 1865–1875 (2003).

56. J. Hu, P. D. Asimow, Y. Liu, C. Ma, Shock-recovered maskelynite indicates low-pressure ejection of shergottites from Mars. *Sci. Adv.* **9**, eadf2906 (2023).

57. B. C. Johnson, G. S. Collins, D. A. Minton, T. J. Bowling, B. M. Simonson, M. T. Zuber, Spherule layers, crater scaling laws, and the population of ancient terrestrial impactors. *Icarus* **271**, 350–359 (2016).

58. R. J. Pike, Formation of complex impact craters: Evidence from Mars and other planets. *Icarus* **43**, 1–19 (1980).

59. L. L. Tornabene, Updated database of craters on Mars with pitted impact deposits (2023); https://doi.org/10.5281/zenodo.8360890.

60. H. G. Sizemore, B. E. Schmidt, D. A. Buczkowski, M. M. Sori, J. C. Castillo-Rogez, D. C. Berman, C. Ahrens, H. T. Chilton, K. H. G. Hughson, K. Duarte, K. A. Otto, M. T. Bland, A. Neesemann, J. E. C. Scully, D. A. Crown, S. C. Mest, D. A. Williams, T. Platz, P. Schenk, M. E. Landis, S. Marchi, N. Schorghofer, L. C. Quick, T. H. Prettyman, M. C. De Sanctis, A. Nass, G. Thangjam, A. Nathues, C. T. Russell, C. A. Raymond, A global inventory of ice-related morphological features on dwarf planet ceres: Implications for the evolution and current state of the cryosphere. *J. Geophys. Res.* **124**, 1650–1689 (2019).

61. A. I. Sheen, Martian meteorite ejection ages compilation (2023); https://doi.org/10.5281/zenodo.10028640.

62. H. Y. McSween, E. Jarosewich, Petrogenesis of the elephant Moraine A79001 meteorite: Multiple magma pulses on the shergottite parent body. *Geochim. Cosmochim. Acta* **47**, 1501–1513 (1983).

63. Y. Liu, Y. Chen, Y. Guan, C. Ma, G. R. Rossman, J. M. Eiler, Y. Zhang, Impact-melt hygrometer for Mars: The case of shergottite Elephant Moraine (EETA) 79001. *Earth Planet. Sci. Lett.* **490**, 206–215 (2018).

64. Q. Zhou, C. D. K. Herd, Q.-Z. Yin, X.-H. Li, F.-Y. Wu, Q.-L. Li, Y. Liu, G.-Q. Tang, T. J. McCoy, Geochronology of the Martian meteorite Zagami revealed by U–Pb ion probe dating of accessory minerals. *Earth Planet. Sci. Lett.* **374**, 156–163 (2013).

65. P. H. Warren, J. P. Greenwood, A. E. Rubin, Los Angeles: A tale of two stones. *Meteorit. Planet. Sci.* **39**, 137–156 (2004).

66. Y. Liu, I. P. Baziotis, P. D. Asimow, R. J. Bodnar, L. A. Taylor, Mineral chemistry of the Tissint meteorite: Indications of two-stage crystallization in a closed system. *Meteorit. Planet. Sci.* **51**, 2293–2315 (2016).

67. C. R. Kuchka, C. D. K. Herd, E. L. Walton, Y. Guan, Y. Liu, Martian low-temperature alteration materials in shock-melt pockets in Tissint: Constraints on their preservation in shergottite meteorites. *Geochim. Cosmochim. Acta* **210**, 228–246 (2017).

68. R. H. Hewins, M. Humayun, J. A. Barrat, B. Zanda, J. P. Lorand, S. Pont, N. Assayag, P. Cartigny, S. Yang, V. Sautter, Northwest Africa 8694, a ferroan chassignite: Bridging the gap between nakhlites and chassignites. *Geochim. Cosmochim. Acta* **282**, 201–226 (2020).

69. J. J. Bellucci, C. D. K. Herd, M. J. Whitehouse, A. A. Nemchin, G. G. Kenny, R. E. Merle, Insights into the chemical diversity of the martian mantle from the Pb isotope systematics of shergottite Northwest Africa 8159. *Chem. Geol.* **545**, 119638 (2020).

70. L. E. Nyquist, D. D. Bogard, C. Y. Shih, J. Park, Y. D. Reese, A. J. Irving, Concordant Rb–Sr, Sm–Nd, and Ar–Ar ages for Northwest Africa 1460: A 346Ma old basaltic shergottite related to "lherzolitic" shergottites. *Geochim. Cosmochim. Acta* **73**, 4288–4309 (2009).

71. J. J. Bellucci, A. A. Nemchin, M. J. Whitehouse, J. F. Snape, R. B. Kielman, P. A. Bland, G. K. Benedix, A Pb isotopic resolution to the Martian meteorite age paradox. *Earth Planet. Sci. Lett.* **433**, 241–248 (2016).

72. W. K. Hartmann, G. Neukum, Cratering chronology and the evolution of Mars. *Space Sci. Rev.* **96**, 165–194 (2001).

73. G. F. Herzog, M. W. Caffee, Cosmic-ray exposure ages of meteorites in *Treatise on geochemistry* (Second Edition), H. D. Holland, K. K. Turekian, Eds. (Elsevier, Oxford, 2014), pp. 419–454.

74. C. D. K. Herd, Insights into the petrogenetic history of the Northwest Africa 7635 augite-rich shergottite. *Meteorit. Planet. Sci.* **58**, 158–164 (2023).

75. R. R. Rahib, A. Udry, G. H. Howarth, J. Gross, M. Paquet, L. M. Combs, D. L. Laczniak, J. M. D. Day, Mantle source to near-surface emplacement of enriched and intermediate poikilitic shergottites in Mars. *Geochim. Cosmochim. Acta* **266**, 463–496 (2019).

76. D. Krietsch, "Alteration on asteroids, diversity of primordial volatiles and their carriers in carbonaceous chondrites, and martian shergottite sampling sites—Studied by meteoritic noble gases," thesis, ETH Zurich, Zurich, Switzerland (2020).

77. T. V. Kizovski, K. T. Tait, V. E. Di Cecco, L. F. White, D. E. Moser, Detailed mineralogy and petrology of highly shocked poikilitic shergottite Northwest Africa 6342. *Meteorit. Planet. Sci.* **54**, 768–784 (2019).

78. A. H. Treiman, The nakhlite meteorites: Augite-rich igneous rocks from Mars. *Chemistry* **65**, 203–270 (2005).

79. A. Udry, J. M. D. Day, 1.34 billion-year-old magmatism on Mars evaluated from the co-genetic nakhlite and chassignite meteorites. *Geochim. Cosmochim. Acta* **238**, 292–315 (2018).

80. G. G. Michael, G. Neukum, Planetary surface dating from crater size–frequency distribution measurements: Partial resurfacing events and statistical age uncertainty. *Earth Planet. Sci. Lett.* **294**, 223–229 (2010).

81. R. Arvidson, J. Boyce, C. Chapman, Standard techniques for presentation and analysis of crater size-frequency data. *Icarus* **37**, 467–474 (1979).

82. G. G. Michael, T. Kneissl, A. Neesemann, Planetary surface dating from crater size-frequency distribution measurements: Poisson timing analysis. *Icarus* **277**, 279–285 (2016).

83. B. S. Preblich, A. S. McEwen, D. M. Studer, Mapping rays and secondary craters from the Martian crater Zunil. *J. Geophys. Res.* **112**, 2006JE002817 (2007).

84. J. R. Hill, P. R. Christensen, Well-preserved low thermal inertia ejecta deposits surrounding young secondary impact craters on Mars. *J. Geophys. Res.* **122**, 1276–1299 (2017).

85. K. Nagao, J. Park, J. Choi, J. M. Baek, M. K. Haba, T. Mikouchi, M. E. Zolensky, G. F. Herzog, C. Park, J. I. Lee, M. J. Lee, Genetic relationship between martian chassignites and Nakhlites Revealed from Noble Gases, in *82nd Annual Meeting of the Meteoritical Society* (LPI Contribution, Sapporo, Hokkaido, Japan, 2019).

86. S. J. K. Symes, L. E. Borg, C. K. Shearer, A. J. Irving, The age of the martian meteorite Northwest Africa 1195 and the differentiation history of the shergottites. *Geochim. Cosmochim. Acta* **72**, 1696–1710 (2008).

87. T. Schulz, P. P. Povinec, L. Ferrière, A. J. T. Jull, A. Kováčik, I. Sýkora, J. Tusch, C. Münker, D. Topa, C. Koeberl, The history of the Tissint meteorite, from its crystallization on Mars to its exposure in space: New geochemical, isotopic, and cosmogenic nuclide data. *Meteorit. Planet. Sci.* **55**, 294–311 (2020).

88. K. Misawa, J. Park, C. Y. Shih, Y. Reese, D. D. Bogard, L. E. Nyquist, Rb–Sr, Sm–Nd, and Ar–Ar isotopic systematics of lherzolitic shergottite Yamato 000097. *Polar Sci.* **2**, 163–174 (2008).

89. M. Righter, T. J. Lapen, A. J. Irving, Sm-Nd and Lu-Hf isotopic systematics of shock-melted intermediate olivine gabbroic Shergottite Northwest Africa, in *50th Lunar and Planetary Science Conference*, (Lunar and Planetary Institute, The Woodlands, TX, 2019).

90. T. Liu, C. Li, Y. Lin, Rb-Sr and Sm-Nd isotopic systematics of the lherzolitic shergottite GRV 99027. *Meteorit. Planet. Sci.* **46**, 681–689 (2011).

91. C.-Y. Shih, L. E. Nyquist, Y. Reese, A. Jambon, Sm-Nd isotopic studies of two Nakhlites, NWA 5790 and Nakhla, in *41st Lunar and Planetary Science Conference*, (Lunar and Planetary Institute, The Woodlands, TX, 2010).

92. L. E. Borg, L. E. Nyquist, Y. Reese, H. Wiesmann, C.-Y. Shih, M. Ivanova, M. A. Nazarov, L. A. Taylor, The age of Dhofar 019 and its relationship to the other martian meteorites, in *32nd Lunar and Planetary Science Conference*, (Lunar and Planetary Institute, The Woodlands, TX, 12 to 16 March 2001).

93. M. Righter, T. J. Lapen, A. J. Irving, Extending the range in ages and source compositions of Shergottites: Lu-Hf and Sm-Nd Age and isotope systematics of Northwest Africa, in *49th Lunar and Planetary Science Conference*, (Lunar and Planetary Institute, The Woodlands, TX, 2018), p. 2609.